

STRUCTURE OF Ag (111) SURFACE BY LOW TEMPERATURE SCANNING TUNNELING MICROSCOPY (LT-STM)

DÜŞÜK SICAKLIK TARAMALI TÜNELLEME MİKROSKOBUNDA Ag (111)'İN YÜZEY ANALİZİ

Asim MANTARCI*

*Muş Alparslan Üniversitesi Fen Edebiyat Fakültesi Fizik Bölümü 49250 Muş

ABSTRACT

In this research, aim is to deeply explore Ag (111) surface, both theoretically and experimentally. Low temperature scanning tunneling microscopes (LT-STM) for experimental study and STMAFM computer program for theoretical aspect were used to analyze Ag (111) surface, as methods. In doing so, LT-STM was correctly set up in the UHV regime; designed all other equipment (the tip, a low noise high voltage amplifier) to resolve nano scale surface structure. A detailed investigation about Ag (111) surface is carried out 5 K and some images were taken by STM. Also STMAFM computer program is used for calculating the distance between Ag atoms. Then it is surely confirmed that experimental data complies with theoretical data. This study is crucial and filled scientific gap because possible application is future spintronic devices. The unique ability of the scanning tunneling microscope to manipulate atoms in a controlled manner provides a possible method for “bottom-up” nanochip design, producing information processors a thousand times smaller than conventional chip packages.

Key Words: *Low temperature scanning tunneling microscopy (LT-STM), Ag (111) surface*

ÖZET

Bu makalede, Ag (111) yüzeyi deneysel ve teorik olarak detaylı şekilde araştırılmıştır. Deneysel çalışma için düşük sıcaklık taramalı tünelleme mikroskopu ve teorik çalışma için STMAFM bilgisayar programı metotları kullanılmıştır. Bunun için nano boyutta veri almak için LT-STM ultra vakum şartlarında doğru bir şekilde kurulmuş ve diğer ekipmanlar dizayn edilmiştir. Deneysel işlemlerle Ag (111) yüzeyinden alınan veriler 5 K de şartlarında alınmıştır. Taramalı tünelleme mikroskopunun çalışması için gerekli karmaşık ekipmanlar ve bu ekipmanların nasıl kurulduğu ve ses ve sinyal izolasyonunun nasıl sağlandığı ve taramalı tünelleme mikroskopunun bir malzeme incelerken nasıl çalıştırıldığı detaylı olarak laboratuvarında yapılmıştır. Atomik olarak temizlenmiş Ag (111) yüzeyinden alınan bu veriler analiz edilmiştir. Bunun yanı sıra STMAFM bilgisayar programı yardımıyla Ag atomları arasındaki mesafe teorik olarak hesaplanacak ve analizi yapılacak ve bunun deneyle tam uyum gösterdiği gösterilecektir. Bu çalışma gelecekteki spintronik aygıtların uygulamasına temel olarak, bilimsel boşluğu doldurduğundan önem arz etmektedir. Ayrıca, STM'in atomik ölçekte atomları kontrol etmesiyle, bottom-up nanochip tasarımında, daha küçük ölçekte nanochip dizayn etme yolu açılacaktır.

Anahtar Kelimeler: *Düşük sıcaklık taramalı tünelleme mikroskopu, Ag (111) yüzeyi*

*Sorumlu Yazar/Corresponding Author: Asim Mantarcı, Muş Alparslan Üniversitesi, Fen Edebiyat Fakültesi, Fizik Bölümü 49250 Muş, E-mail: a.mantarci@alparslan.edu.tr

1. INTRODUCTION

1.1. How STM (Scanning Tunneling Microscopy) Works

Scanning tunneling microscopy, invented in 1981 by Gerd Binnig and Heinrich Rohrer, is one of only a handful of microscopy techniques capable of resolution from atomic to micrometer scales [1]. The operation principle of STM is based on the quantum mechanical phenomena called tunneling. Let us consider that we have a particle that has energy E and potential barrier V . Classically mechanically speaking, if the particle has an energy E less than potential barrier V , this particle will not penetrate the barrier. We can think of this situation as the ball hitting the wall and coming back, a very simple example from our daily life. According to quantum mechanics, this situation changed in 1896, since Henri Becquerel discovered quantum tunneling by studying radioactivity decaying. If the particle has an energy E less than potential barrier V , the particle will have a finite possibility of penetrating the barrier. Take an electron as a particle. According to quantum mechanics, an electron has a wave function that describes its motions in all regions of space. In detail, quantum tunneling can be explained by considering an electron incident from the $-x$ direction on a one dimensional rectangular barrier, illustrated in Figure.1.

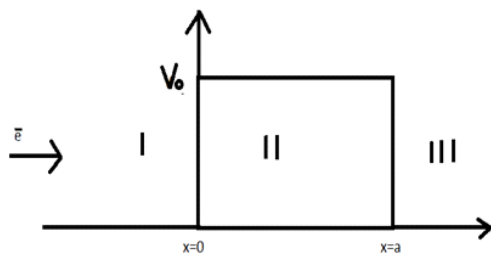


Figure 1. One dimensional rectangular barrier.

Quantum mechanics says that there is a finite probability that it will tunnel through the barrier and emerge on the other side. We can think of three regions: region I, region II and region III. By using quantum mechanics principles, the wave function in each region is calculated by the Schrödinger equation.

$$H\Psi = E\Psi \quad (1)$$

In this equation, H is a system of Hamiltonian, ψ is a wave function, and E is the energy of the system. We can also obtain wave function for every region with the following equations;

$$\begin{aligned} \psi_I &= B_I e^{ik_1x} + C_I e^{-ik_1x} \\ \psi_{II} &= B_{II} e^{k_2x} + C_{II} e^{-k_2x} \\ \psi_{III} &= B_{III} e^{ik_1x} + C_{III} e^{-ik_1x} \end{aligned} \quad (2)$$

Where $k_1 = \sqrt{\frac{2mE}{\hbar^2}}, k_2 = \sqrt{\frac{2m(V_0-E)}{\hbar^2}}$

B_I is the incident wave amplitude, C_I the reflected wave amplitude, and B_{III} is the transmitted wave amplitude. To calculate the probability of reflection and transmission, we should apply boundary condition to the system. Boundary conditions are following:

$$\psi_I(x=0) = \psi_{II}(x=0) \quad (3)$$

$$\psi'_I(x=0) = \psi'_{II}(x=0) \quad (4)$$

$$\psi_{II}(x=a) = \psi_{III}(x=a) \quad (5)$$

$$\psi'_{II}(x=a) = \psi'_{III}(x=a) \quad (6)$$

("' "Denotes derivative with respect to x)

Transmission coefficient, which is $T = \left| \frac{B_{III}}{B_I} \right|^2$ (7)

and reflection coefficient, which is $R = \left| \frac{C_I}{B_I} \right|^2$ (8) can be calculated by using the above four equations having four unknowns, and considering $R + T = 1$ (9)

After some algebra, T can be found, which is the transmission coefficient that is important for relating the magnitude of the probability of the tunneling, given by

$$T = \frac{1}{1 + \frac{V_0^2}{4E(V_0-E)} \sinh^2(ak_2)} \quad (10)$$

If we apply limiting case $a \sqrt{\frac{2m}{\hbar^2} (V_0 - E)} \gg 1$ we can consider that

$$\sinh^2(ak_2) \rightarrow \frac{1}{4} e^{2ak_2} \quad (11)$$

In the equation (2), 1 can be ignored since $ak_2 \gg 1$; then transmission coefficient becomes

$$T \approx \frac{16E(V_0-E)}{V_0^2} e^{-2k_2a}. \quad (12)$$

This formula tells us that transmission coefficient is proportional to exponential decaying with a thickness of barrier. Quantum tunneling is of great importance to contribute developing technology and has a lot of applications; for instance, α -decay. Tunneling in occurs in α -decay, allowing α -particles to tunnel out of unstable nuclei. [2] Another application of the quantum tunneling is called cold emission; that is, if a metal is placed in very strong field, it forms a cathode; then the electrons are emitted from the surface of the metal. [3] Also, one of the significant applications of the tunneling is the scanning tunneling microscopy (STM). It is a machine that can obtain images from the surface of the material at the atomic level and also can be used for atomic manipulations. If we would like to see one of the sections of the STM that allows us to take images and do atomic manipulation, we mainly find the important parts; the tip and sample. When we want to understand the relationship between STM and quantum tunneling phenomena, we should consider the potential barrier to be the vacuum gap between the tip and the sample. In addition, we can think of the first and third region mentioned above as a tip and sample depending on applied voltage. We can illustrate in figure [1.2]

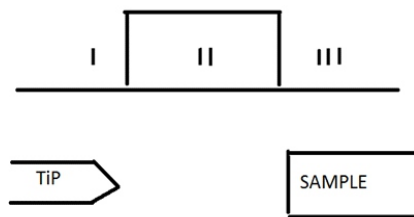


Figure 2. Illustration of quantum tunneling with tip and sample.

When we apply negative voltage to the sample, the sample is going to be negative with respect to the tip and the electrons are going to tunnel from the sample to the tip. In the case of applying positive voltage to the sample, the sample is going to be positive with respect to the tip and the electrons are going to tunnel from the tip to the sample. These are illustrated in fig. [1.3] and [1.4]

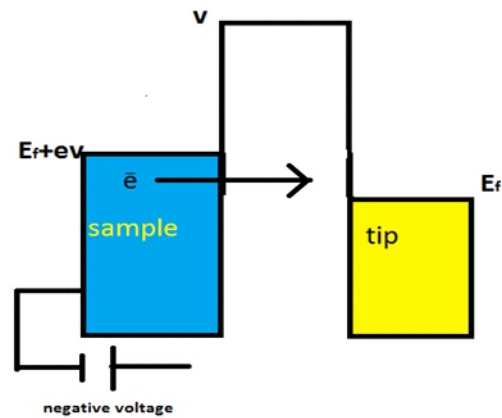


Figure 3. Tunneling through from the sample to the tip

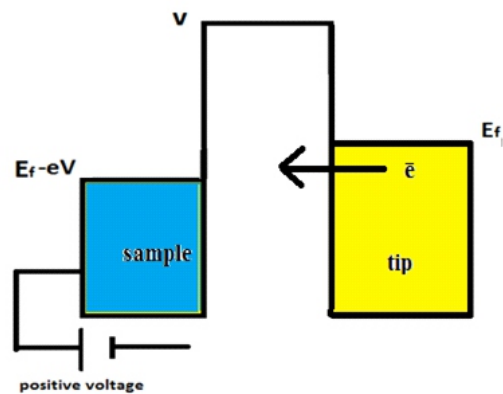


Figure 4. Tunneling through from the tip to the

In both cases of applying negative and positive voltage to the sample, there will be electrons flowing through from the tip to the sample and vice versa. Flowing electrons is going to be the cause of a small current. This is known as tunneling current. Since quantum mechanical tunneling theory is governing the interaction between the tip and surface, the transmission coefficient that describes the probability of an electron tunneling through a barrier, (in our case barrier is the gap between the tip and sample), is proportional to the tunneling current. Based upon quantum tunneling and tunneling current mentioned above, we can explain metal-vacuum-metal tunneling as shown in figure [1.5].sample

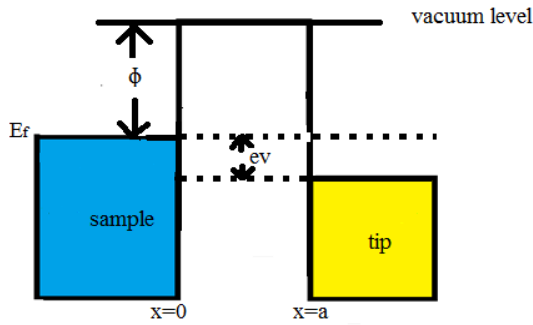


Figure 5. A one-dimensional metal-vacuum-metal tunneling junction (This figure was taken from the book is Introduction to Scanning Tunneling Microscopy, Chen, C. Julian, 2008)

The work function (ϕ) of a metal surface is defined as the minimum energy required for removing an electron from the bulk to the vacuum level [1]. If assumed that the sample and tip has the same work function (ϕ) and they are made of the same material, also neglecting thermal excitation, the Fermi energy E_f is equal to $-\phi$ [1]. Tunneling current is directly proportional to the probability W for an electron in the n th sample state to present at the tip surface; $x=a$, is

$$W \approx |\psi_n|^2 e^{-2ka} \quad (13)$$

By including all the sample states in the energy interval eV , tunneling current becomes proportional to

$$I \approx \sum_{E_n=E_f-eV}^{E_f} |\psi_n|^2 e^{-2ka} \quad (14)$$

Where $k = \frac{\sqrt{2m\phi}}{\hbar}$ and ψ_n is the value of the n th sample state at the sample surface

Local density of states that is defined as the number of electron per unit volume per unit energy through the region from $E_f - \varepsilon V$ to E_f and, at a location x and energy E can be written [1],

$$\rho_s(x, E) = \frac{1}{\varepsilon} \sum_{E_n=E-\varepsilon}^E |\psi_n|^2 \quad (15)$$

For a small ε . Then, tunneling current becomes,

$$I \approx V \cdot \rho_s(0, E) e^{-2ka} \quad (16)$$

Now, we have the relationship that the tunneling current is proportional to applied voltage and local density of states and exponentially

2. MATERIAL AND METHOD

2.1. Instrumentation of the Scanning Tunneling Microscopy (STM)

2.1.1. Ultra-High-Vacuum Chamber

Ultra high vacuum is an essential requirement in all studies of clean surfaces using for example the techniques of field-electron and field-ion microscopy, scanning tunneling microscopy (STM), electron diffraction, Auger electron spectroscopy, secondary ion mass spectrometry and photoelectron spectroscopy and it has the range

In both cases of applying negative and positive voltage to the sample, there will be electrons flowing through from the tip to the sample and vice versa. Flowing electrons is going to be the cause of a small current. This is known as tunneling current. Since quantum mechanical tunneling theory is governing the interaction between the tip and surface, the transmission coefficient that describes the probability of an electron tunneling through a barrier, (in our case barrier is the gap between the tip and sample), is proportional to the tunneling current. Based upon quantum tunneling and tunneling current mentioned above, we can explain metal-vacuum-metal tunneling as shown in Figure 5.

ultra high vacuum (UHV) chamber that consists of three sections: the STM and the cryostat chamber, the preparation chamber, and the load-lock chamber.

2.1.2. STM and Cryostat Chamber

The first section of the UHV system is the STM and cryostat chamber. The cryostat is a bathycryostat that has inner and outer coolant containers. The outer container is filled with liquid nitrogen, which also acts as a thermal radiation shield. The inner container is filled with liquid helium. It is illustrated in Figure 6.

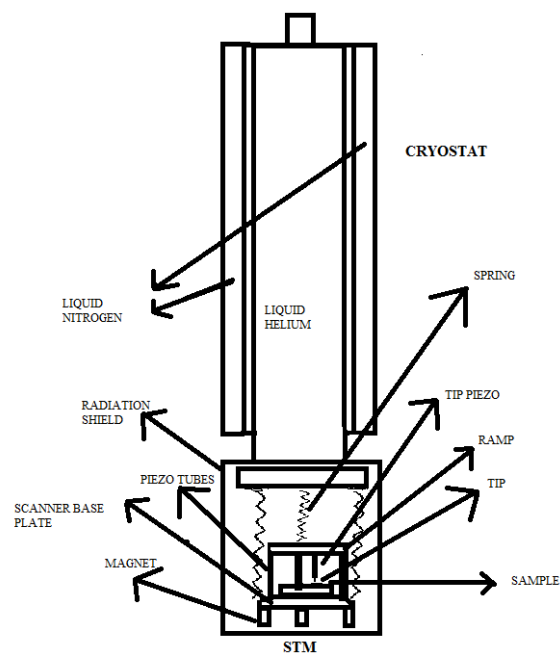


Figure 6. Illustration of STM and cryostat chamber.

The STM chamber is attached to the inner cryostat and has an STM scanner that is hung up with three springs. It is thermally shielded to prevent electromagnetic radiation. The STM is a modified Besocke-Beetle type scanner [5], which consists of a ramp, tip piezo, tip and three piezoelectric tubes which allow the tip to approach to the sample properly. This approaching process is done by rotating the ramp. A piezoelectric actuator is an electromechanical device that undergoes a dimensional change when electric voltage is applied [6]. So, three piezoelectric tubes allow the tip to be properly moved across the surface, and they are used in scanning over a surface.

There is another piezo attached to the tip, called the tip piezo. If positive voltage is applied to it, the tip piezo will be lengthened. If negative voltage is applied to it, the tip piezo will be shortened. This allows us to have control of tip sample distance in z direction. In an STM experiment, the tip is a crucial issue for scientists since the size, shape and chemical identity of the tunneling tip influence not only the resolution and shape of the STM scan, but also the measured electronic structure [6]. Because of that, it is a requirement to have a very stable and sharp tip for the experiment that needs to be done well. STM tips are typically fabricated from

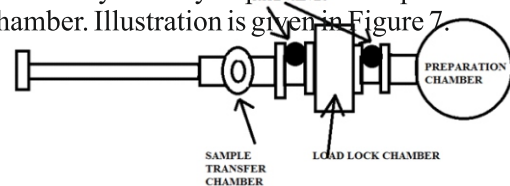
metal wires of tungsten (W), platinum–iridium (Pt-Ir), or gold (Au) and sharpened by mechanical grinding, cutting with a wire cutter or razor blade, 'controlled' crashing, field emission/evaporation, ion milling, fracturing, or electrochemical etching [6].

2.1.3. Preparation Chamber

The second section of the UHV chamber is the preparation chamber, the largest part of the machine. Main purpose of this chamber is to allow us to have the sample prepared before moving it into the STM. UHV gauges, ion pump, titanium sublimation pump (TSP), sputtering gun, sample storage unit and the manipulator are the parts that belong to the preparation chamber. Mainly, we are using the preparation chamber for cleaning the sample and depositing atoms or molecules on the sample's surface. Cleaning is an experimental procedure that has two main processes: sputtering and annealing. The sample surface may have attached gas molecules. The sputtering process can be done by bombarding the sample with high energy neon ions in order to remove undesired contamination like sticking gas molecules on the surface. When the surface is hit by high energy neon, it becomes rough. To have a smooth surface, the annealing process should be done by heating the sample to a high temperature.

Load-Lock Chamber

The third part of the UHV chamber is the load lock chamber. One side opens to the preparation chamber. The other side is connected with the sample transfer chamber. The load lock chamber is used for allowing us to have the sample and other tools transferred to the preparation chamber without venting the whole chamber. By using the load lock chamber, we can make small repairs, and change the sample or tip without needing to vent the entire system. Also, grown sample can be transferred into the system by a portable sample transfer chamber. Illustration is given in Figure 7.



2.1.4. Pumps

To achieve and maintain the ultra high vacuum's pressure, several kinds of pumps can be used, for example, rotary (roughing) pump, turbo molecular pump, ion pump, titanium sublimation pump (TSP), and cryopump.

2.1.4.1. Rotary (roughing) pump

The term 'rough vacuum' usually refers to the pressure region between atmospheric pressure and 1×10^{-3} torr [7]. A single stage oil sealed rotary pump can produce inlet pressure near 0.010 torr for air while discharging the atmosphere [7]. Modern two stages rotary pump can produce at the inlet a partial pressure of air below 1×10^{-5} torr [7]. The rotary pump is the initial pump of the system and starting the pumping of the vacuum chamber can be done by the rotary (roughing) pump.

2.1.4.1.1. Turbo molecular pump

The next pumping step is the turbo molecular pump which is capable of reaching a pressure of 10^{-9} torr. Turbo molecular pumps transport gases by applying a mechanical momentum to the gas particle, which is directed toward the outlet of the pump [8].

2.1.4.1.2. Ion pump

Ion pump is the significant pump inside the preparation chamber which we are using to reach and maintain the UHV pressure of 10^{-11} torr. It can be used when we have a pressure below 10^{-6} torr. The ion pump is very suitable for STM because it has no moving parts, which can give rise to vibration. Minimizing vibration is crucial for STM experiment because any vibration can overpower the signal coming in.

2.1.4.2. Titanium sublimation pump (TSP)

A titanium sublimation pump can also be used with the ion pump and turbo molecular pump. Titanium is the choice for commercial pumps because it can be sublimed (changed from the solid to vapor state without being a liquid) at much lower temperatures than most other metals, is inexpensive, and pumps a large

number of gases [9]. Like the ion pump, TSP also has no moving parts which produce vibration. Therefore, TSP is a good pump for STM experiments.

2.1.4.3. Cryopump

A cryostat can be used as a cryopump as it produces a low pressure vacuum by condensing vapors on its very low temperature cold surface. Like TSP and the ion pump, the cryopump does not have moving parts which cause vibration. It is also suitable for STM experiments.

2.1.5 Tip Preparation/Formation

One of the important components of the STM is the quality of the tip. In order to get reliable data, a good tip is necessary. An ideal tip has exactly one atom at the end. A common way to prepare a tip is by an electrochemical etching of a polycrystalline tungsten wire. Other types of tip, like Pt-Ir, can be made by cutting and pulling the wire. A very sharp tip can be made by this method as well. Once a sharp tip is achieved, it can be further improved by in-situ tip preparation [15]. In this technique, the STM tip is brought to very close to the substrate and crashed gently on the surface. The tip surface mechanical contact produces local heat, which reshapes of the tip apex into a sharper profile.

3. RESULTS

3.1 Some Images Were Taken By Using STM

I took some images from the Ag (111) sample surface. To find the image size of each image, the calibration is needed. It is done by utilizing that the distance between two atoms is 2.89 \AA for the Ag (111) surface. In detail, STMAFM computer program is used for calibration process. First we need to do is to choose one image that is capable of clearly seeing two atomic distance. In this image, if we draw a line between two or more atoms, we can have the distance between two atoms with helping the program. The distance that is found might be different from the value 2.89 \AA . Now, we have to need to calibrate it by going to the 'panel' in the parameter section and

changing the value of $X_{Piezoconst}$ and $Y_{Piezoconst}$. We should continue this process until we have the value of 2.89 \AA as a distance between two atoms. After several attempts, when we plug into the value of 145 to $X_{Piezoconst}$ and 145 to $Y_{Piezoconst}$, distance between two atoms, which is 2.89 \AA , is found. Therefore, calibration is completed.

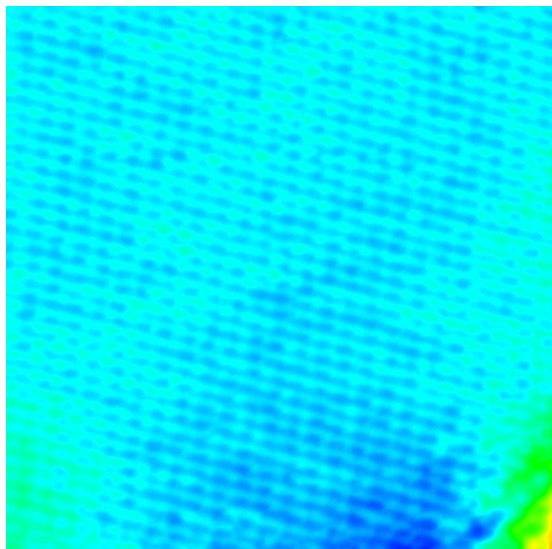
Now, we should find the image size for every image. In the laboratory, we are using the table of reference image size. The table is adjusted by considering our data, it is given by:

1 × 1, 3,3,3; 512 × 512	> 6.797 × 6.797 nm
2 × 2, 3,3,3; 512 × 512	> 13.594 × 13.594 nm
4 × 4, 3,3,3; 512 × 512	> 27.188 × 27.188 nm
8 × 8, 3,3,3; 512 × 512	> 54.376 × 54.376 nm
16 × 16, 3,3,3; 512 × 512	> 108.752 × 108.752 nm
32 × 32, 3,3,3; 512 × 512	> 217.504 × 217.504 nm
64 × 64, 3,3,3; 512 × 512	> 435.008 × 435.008 nm

(This table was taken from surface science laboratory- Department of Physics and Astronomy at Ohio University, Ref. Image B071031.160140)

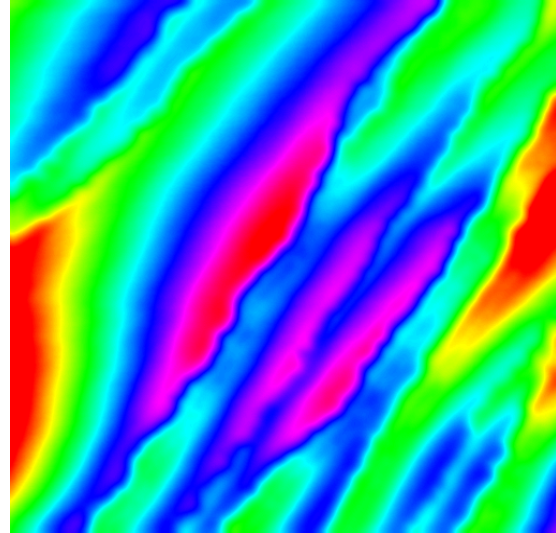
By using this table and STMAFM program' data, we can have the image size for every image.

In the first image, 50 mV voltages is applied and the tunneling current is $1.0 \times 10^{-10} \text{ A}$ and the image size is $6.797 \times 6.797 \text{ nm}$. First image is given by:



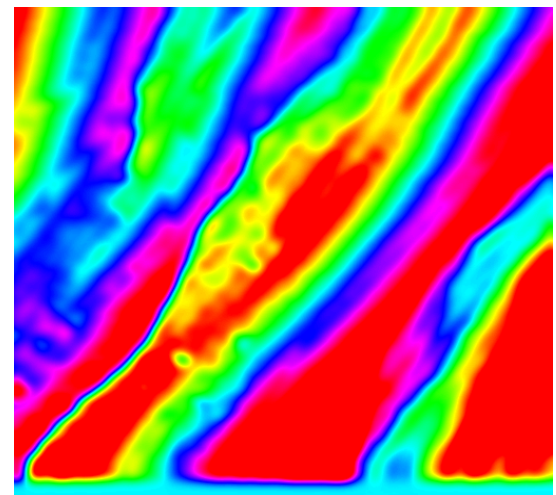
$I=1.0 \times 10^{-10} \text{ A}$, $V=50 \text{ mV}$, the sample is Ag (111) surface, the image size is $6.797 \times 6.797 \text{ nm}$

For the next image, applied voltage is 100 mV, the tunneling current is $2.4 \times 10^{-10} \text{ A}$, and the image size is $54.376 \times 54.376 \text{ nm}$. It is given by:



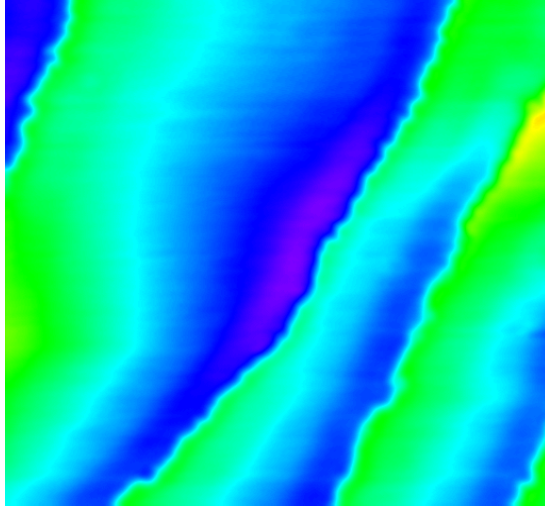
$I=2.4 \times 10^{-10} \text{ A}$, $V=100 \text{ mV}$, the sample is Ag (111) surface, the image size is $54.376 \times 54.376 \text{ nm}$

For another image, applied voltage is 101.9 mV the tunneling current is $2.4 \times 10^{-10} \text{ A}$, and the image size is $217.504 \times 217.504 \text{ nm}$. It is given by:



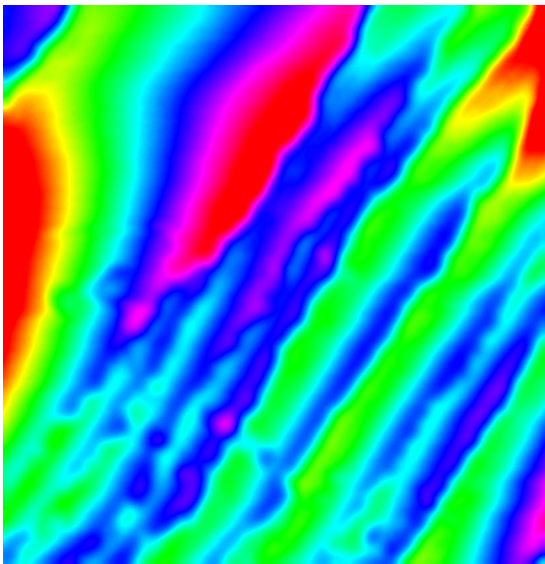
$I=2.4 \times 10^{-10} \text{ A}$, $V=101.9 \text{ mV}$, the sample is Ag (111) surface, the image size is $217.504 \times 217.504 \text{ nm}$

For another image, applied voltage is 40 mV, the tunneling current is 1.1×10^{-9} A, and the image is 54.376 x 54.376 nm. It is given by:



$I=1.1 \times 10^{-9}$ A, $V=40$ mV, the sample is Ag (111) surface, the image size is 54.376 x 54.376 nm

For another image, applied voltage is 100 mV, the tunneling current is 6.0×10^{-10} A tunneling current is image size is 54.376 x 54.376 nm. It is given by:



$I=6.0 \times 10^{-10}$ A, $V=100$ mV, the sample is Ag (111) surface, The image size is

3.2 Overview of the Ag (111) Surface Properties

Silver (Ag) is one of the precious metals, which is widely used for centuries due its noble character. From the application point of view, it has various useful properties such as high electrical and thermal conductivities, and optical reflectivity etc. It is also used for various purposes such as catalytic reactions, photographic films, or photo sensitive materials. From the research point of view, it is one of the clean materials, which can be used as a model system to compare the results between theories and experiments.

Ag (111) surface is one of the two main substrates studied in this work. The surface with (111) orientation is mostly preferred due to the nearly free electron states. The existence of surface states on the noble metal surfaces provides an excellent model system to study about the propagation of electron gas in 2D system. STM can be used as a unique tool to probe such states on the atomic scale. The ability of STM to manipulate atoms on the surfaces, confining them in some geometrical shapes, and probing its electronic properties may provide useful information for future nanotechnology applications [14]. Lately, many researchers have studied Silver (Ag) surface with different their view. One of the researches is that focuses on the geometric and electronic structures of silicene grown on Ag (111) investigated by scanning tunneling microscopy (STM), low energy electron diffraction (LEED) and density functional theory (DFT) calculations. And, the silicene on Ag (111) takes locally-buckled structure in which the Si atoms are displaced perpendicularly to the basal plane [16]. Another study is about the $\sqrt{3} \times \sqrt{3}$ reconstruction is mainly determined by the interaction between Si atoms and have weak influence from Ag substrate. The proposed mechanism opens the path to understanding of multilayer silicon [17]. Other significant research was done is about the existence of Dirac fermion in silicene on Ag(111) surface with $(\sqrt{3} \times \sqrt{3})R30^\circ$ superstructure has been proven by the observation of linear energy-momentum dispersion and quasiparticle chirality by scanning tunneling microscopy (STM) and

spectroscopy (STS) [18].

3.2 Data Analysis

In this section we will analyze and discuss quantitative results of STM imaging and atomic manipulation. This entire process takes place inside of the STM system described in previous chapters, on a sample surface of Ag (111) at liquid helium temperatures. We approach, in constant-current mode, with the bias voltage between the tip and substrate of 40 mV- 50 mV - 100 mV- $V=101.9$ mV, with the tunneling current of them. At this stage, we begin to scan sample surface. In the first image, every blue spot represents Ag atom. We studied in the fcc (111) means atoms are arranged at the corners and center of each cube face of the cell. The fcc (111) materials such as Ag have a hexagonal arrangement of atoms. In case of Ag (111), the nearest neighbor atom distance along this direction is 2.89 \AA and the close-packed rows repeat at every 60 degrees in the surface plane. We wanted to make sure that our images are appropriate, then we checked this distance by using STMAFM computer program. In detail, STMAFM computer program is used for calibration process. First we need to do is to choose one image that is capable of clearly seeing two atomic distance. In this image, if we draw a line between two or more atoms, we can have the distance between two atoms with helping the program. The distance that is found might be different from the value 2.89 \AA . Now, we have to need to calibrate it by going to the 'panel' in the parameter section and changing the value of XPiezoconst and YPiezoconst. We should continue this process until we have the value of 2.89 \AA as a distance between two atoms. After several attempts, when we plug into the value of 145 to XPiezoconst and 145 to YPiezoconst, distance between two atoms, which is 2.89 \AA , is found. Therefore, calibration is completed. We surely confirmed that our analysis is correct and our images are appropriate.

4. CONCLUSIONS

A fully functioning, low temperature scanning tunneling microscope has been constructed, based on the principles of quantum mechanical theory. This STM operates in the UHV regime, with the assistance of a complex arrangement of specialized materials and equipment. A low noise, high voltage amplifier has been designed and built on the exact low noise specifications that the STM demands. The HV-AMP controls the tip of the microscope during all operation, and allows a researcher the freedom of manually or automatically approaching a sample surface during experimental procedure. By using the full ability of STM, the image resolution of Ag (111) in a controlled fashion has been conclusively demonstrated. Also, the construction of a LT-STM system for atom manipulation has been conclusively investigated. A detailed investigation about silver (111) surface is carried out 5 K. We approach, in constant-current mode, with the bias voltage between the tip and substrate of 40 mV- 50 mV -100 mV- $V=101.9$ mV, with the tunneling current of them. At this stage, we begin to scan sample surface. Some images were taken by using STM. They were analyzed in terms of structure of surface. It shows some defects on surface. Also, some areas of surfaces were smoother than other. Our results were checked with theoretical result by using STMAFM computer program. Detailed analysis was given in data analysis section. For future direction, metal or semiconductor surface can be used as a substrate to investigate different electronic properties at the atomic scale. Magnetic atoms/molecules can be deposited on the surface at different temperature. Using lateral/vertical manipulations, these can be relocated to the desired locations. LDOS can be measured precisely at those places using lock-in amplifier techniques, which can give important information systems. Various atomic scale structures can be formed by manipulating

interaction. This will be valuable information for future spintronic devices. With the demand for rapid-paced technological advancement increasing every year and extending into all regions of business and private life, soon the size limitations on conventional microchip technology will prove a limiting factor in the speed of informational processing capacities. The unique ability of the scanning tunneling microscope to manipulate atoms in a controlled manner provides a possible method for “bottom-up” nanochip design, producing information processors a thousand times smaller than conventional chip packages. In addition to the aesthetic benefits that may be derived from atomic manipulation, the STM has opened the atomic realm up for scientific scrutiny and will remain invaluable in obtaining and understanding of the nature of physical interactions in their basal form.

REFERENCES

- [1]. Chen, C. Julian., Introduction to Scanning Tunneling Microscopy, New York: Oxford University Press, 2008.
- [2]. John, B., Alan, D., Robert, L., Joy, M., Andrew, N., Quantum Physics of Matter, London: Institute of Physics Publishing, 2000.
- [3]. Mohsen, R., Quantum Theory of Tunneling, Singapore: World Scientific Publishing Co. Pte. Ltd, 2003.
- [4]. Chambers, A., Fitch, R.K., Halliday, B.S., Basic Vacuum Technology, London: Institute of Physics Publishing, 1998.
- [5]. Besocke, K., An Easily Operatable Scanning Tunneling Microscope, *Surface Science*, 181, 145-153, 1987.
- [6]. Chunli, B., Gerhard, E., Robert, G., Hans, L., Douglas, L.M., Scanning Tunneling Microscopy and Its Applications, Shanghai, Shanghai Scientific and Technical Publishers, 1992.
- [7]. Hablanian, M.H., High-Vacuum Technology, A Practical Guide, New York: Marcel Dekker, Inc., 1997.
- [8]. Karl, J., Handbook of Vacuum Technology, Weinheim: Verlag GmbH & Co., 2008.
- [9]. F.O'Hanlon, John. A User's Guide to Vacuum Technology, New Jersey: John Wiley&Sons, Inc., 2003.
- [10]. Hla, S-W., Bartels, L., Meyer, G. and Reider K.-H., Inducing All Steps of a Chemical Reaction with the Scanning Tunneling Microscope Tip: Towards Single Molecule Engineering, *Phys. Rev. Lett.* 85, 2777-2780, 2000.
- [11]. Hla, S-W., Scanning Tunneling Microscopy Single Atom/Molecule Manipulation and Its Application to Nanoscience and Technology, *J Vac. Sci & Tech B*, 23, 1251-1360, 2005.
- [12]. Eigler, D.M., and Schweizer, E.K., Positioning Single Atoms with A Scanning Tunneling Microscope, *Nature* 344, 524-526, 1990.
- [13]. Shen, T.C., Atomic-Scale Desorption Through Electronic and Vibrational Excitation Mechanism, *Science*, 268, 1590-1592, 1995.
- [14]. Nilus, N., Wallis, T.M., and Ho, W., Development of One-Dimensional Band Structure in Artificial Gold Chains, *Science*, 297, 1853, 2002.
- [15]. Vacancy scanning tunneling spectroscopy on Ag (111), Poster Presentation, APS March meeting Baltimore, USA, 2006.
- [16]. Noriaki Takagi, C-L.L., Tsukahara, N., Kawai, M., & Arafune, R. Silicene on Ag(111): Geometric and Electronic Structures of a New Honeycomb Material of Si, *Progress in Surface Science*, 1–20, 2015.
- [17]. Seymour Cahangirov, V.O., Atomic Structure of the $\sqrt{3} \times \sqrt{3}$ Phase of Silicene on Ag(111), *Physical Review B*, 1-5, 2014.
- [18]. Wu, K., Persistent Dirac Fermion State in a Silicon-based Material, Program of the 4th ICQs Conference on Spintronics, Beijing, 15, 2014.